COMMUNICATION

Energy-Efficient Dehumidification over Hierachically Porous Metal–Organic Frameworks as Advanced Water Adsorbents

You-Kyong Seo, Ji Woong Yoon, Ji Sun Lee, Young Kyu Hwang, Chul-Ho Jun, Jong-San Chang, Stefan Wuttke, Philippe Bazin, Alexandre Vimont, Marco Daturi, Sandrine Bourrelly, Philip L. Llewellyn, Patricia Horcajada, Christian Serre, and Gérard Férey*

Water sorption technologies are widely used commercially in many contexts, including industrial or indoor desiccant applications such as desiccant dehumidifiers, gas dryers, adsorptive air conditioning systems, fresh water production, adsorption heat transformation, etc.[1] In recent years, the potential for energy savings through improved efficiency has received increased attention, particularly as low-grade thermal energy or solar energy could be utilized. Currently, silica gel and zeolites are widely utilized commercially, often formed into corrugated honeycomb rotors.[1] As these sorbents typically must be heated above 150 °C during the desorption step, these sorbents are far from ideal in terms of energy consumption. There are additional issues with the level of dehumidification that these materials are able to achieve.[1] Improved energy efficiency requires advanced water adsorbents that can be regenerated together with the removal of a large amount of water vapor from humid conditions.[1] If such materials could operate at or below 80 °C, they could utilize readily available waste heat, leading to further energy savings.

Among the existing classes of porous solids, crystalline metal–organic frameworks (MOFs)[2] are currently of great interest and importance due to their novel coordination structures, diverse topologies, and potential applications in the field of separation, gas storage, catalysis, or biomedical applications.[3] In spite of versatile advantages of porous MOFs, which include tailor-made pore structures and controllable porosity by change of organic ligands and metal subunits,[2] most MOFs suffer from a lack of hydrothermal stability.[4] Structural damage to a MOF caused by moisture at processing conditions or during regeneration will strongly limit the utilization of a MOF as a sorbent for industrial applications.[4] Conversely, highly porous MOFs with good hydrothermal stability represent candidates for industrially useful water sorbents. Cubic mesoporous metal(III) di- or tri-carboxylates with hierachical pore structures labeled MIL-101(Cr), MIL-100(Fe), MIL-100(Cr), and MIL-100(Al) (MIL stands for Materials of Institut Lavoisier) using trivalent octahedral metals and the simplest aromatic carboxylates such as terepthalate and trimesate have been discovered.[5,6] Based on this requirement, the exceptional hydrothermal stability and large sorption uptakes known for MIL-101 and MIL-100 encouraged us to assess their applicability for water sorption applications.[5,6] Despite studies done on water adsorption in MOFs,[7] reports dealing with MOFs as water adsorbents are still scarce[8] and there is a particular need to evaluate their low temperature desorption properties, i.e., below 80 °C for application to energy-efficient dehumidication systems. Here, we report an exhaustive analysis of their water sorption properties, revealing their intricate and unique structural properties such as large amounts of sorption, fast sorption rates and fascinating desorption properties that are essential for energy-efficient water sorption applications.

MIL-101(Cr) and MIL-100(Fe) were synthesized through hydrothermal reactions for 8 h at 220 °C and 160 °C, respectively, (see Supporting Information) as reported elsewhere.[6b,6c] Importantly, their crystalline structures are kept intact after exposure to boiling water at 100 °C for 7 days (Figure S1, S2, Supporting Information), giving reproducible proof of their hydrothermal stability.

MIL-101(Cr) and MIL-100(Fe) possess unique sorption properties for water vapor at room temperature and elevated temperature (<80 °C). As shown in Figure S3 (Supporting Information), the water sorption isotherm in MIL-101(Cr) shows a unique shape with an initial adsorption step ($p/p_0 < 0.2$; p_0: saturation vapor pressure) (Figure S3, Supporting Information), indicating the presence of the coordinatively unsaturated chromium sites followed by strong uptakes due to two capillary

Y.-K. Seo, Dr. J. W. Yoon, J. S. Lee, Dr. Y. K. Hwang, Dr. J.-S. Chang
Catalysis Center for Molecular Engineering (CCME)
Korea Research Institute of Chemical Technology (KRICT)
Jang-dong 100, Yuseong, Daejeon 305-600, Korea
E-mail: jschang@krict.re.kr
Y.-K. Seo, J. S. Lee, Prof. C.-H. Jun
Department of Chemistry
Center for Bioactive Molecular Hybrid, Yonsei University
Seodaemoonku, Seoul 120-749, Korea
Dr. S. Wuttke, P. Bazin, Dr. A. Vimont, Prof. M. Daturi
Laboratoire Catalyse et Spectrochimie
UMR 6506, CNRS/ENSICAEN et Université de Caen Basse-Normandie
UNICITE, 14, rue Alfred Kastler
14052 Caen Cedex 4, France
Dr. S. Bourrelly, Dr. P. L. Llewellyn
Laboratoire Chimie Provence
UMR 6264 Universite's Aix-Marseille I, II & III-CNRS
Centre de St Jérôme, 13397 Marseille Cedex 20, France
Dr. S. Wuttke, Dr. P. Horcajada, Dr. C. Serre, Prof. G. Férey
Institut Lavoisier (UMR CNRS 8180)
Université de Versailles Saint-Quentin-en-Yvelines
45 avenue des Etats-Unis
78035 Versailles Cedex, France

DOI: 10.1002/adma.201104084

condensation steps in the mesoporous cages, which is similar to that in MIL-100(Fe) (Figure S3, Supporting Information). This isotherm shape makes the MOF adsorbents special compared to zeolites and silica-gel adsorbents. It is also consistent with their structural features showing two mesoporous cages with two microporous windows. The capillary condensation steps are accompanied by hysteresis loops, which confirm such a condensation mechanism. Adsorption isobars of water vapor in MIL-101(Cr) (BET surface area, S_{BET} = 4150 ± 100 m^2 g^{-1}) (Figure S4, Supporting Information) and MIL-100(Fe) (S_{BET} = 2300 ± 100 m^2 g^{-1}) (Figure S5, Supporting Information) dehydrated at 150 °C for 12 h clearly reveal the dependence of sorption uptakes on adsorption temperature and water vapor pressure. These materials exhibit very high equilibrium uptakes, i.e., >1.5 g g^{-1} for MIL-101(Cr) and >0.84 g g^{-1} for MIL-100(Fe) above 2.4 kPa (p/p_0 = 0.57) at 30 °C. However, their uptakes decrease to less than 0.20 g g^{-1} above 60 °C and below 4.8 kPa (p/p_0 = 0.24).

As expected, water sorption isotherms at 30 °C show outstanding water sorption uptakes of MIL-101(Cr) and MIL-100(Fe) at relatively high partial pressures, p/p_0 > 0.5, i.e., 1.61 g-H_2O per g dry adsorbent for MIL-101(Cr) and 0.873 g H_2O per g dry adsorbent for MIL-100(Fe) (Figure S3, Supporting Information), which are 2.5–5.0 times higher than those of zeolite NaX (0.336 g H_2O per g dry adsorbent), silicoaluminophosphate SAPO-34 (0.330 g H_2O per g dry adsorbent) and silica gel (0.327 g H_2O per g dry adsorbent), which are currently used as commercial water adsorbents (Figure S6,S7, Supporting Information). In addition, other isomorphous phases MIL-100(Cr) and MIL-100(Al) that were synthesized by hydrothermal methods according to the literature[7c,7d] represent the similar sorption uptakes to that of MIL-100(Fe) (Figure S3, Supporting Information). To the best of our knowledge, the equilibrium uptakes (1.50–1.70 g g^{-1}) in dehydrated MIL-101(Cr) at 30–40 °C and p/p_0 > 0.5 would be one of the highest values among those ever reported in solid adsorbents.[1b]

In order to explain the large water uptake observed in these materials, we measured N_2 physisorption isotherms at –196 °C using a volumetric gas sorption apparatus (Figure S8, Supporting Information) on samples activated at 30 °C under vacuum. Despite the low activation temperature, more than 90% of their total pore volumes (based on activation at 150 °C for 1 day) were recovered in both cases. This implies that these materials can be almost fully dehydrated at 30 °C, in contrast to conventional porous materials requiring high temperature dehydration before use. This property is of great importance for energy-efficient dehumidification.

Besides water sorption capacity and hydrothermal stability, sorption kinetics of water vapor and the degree of regeneration (or reversibility) are also important factors that should be taken into consideration for industrial applications.[1b] High sorption rates of water vapor allow faster rotation cycles of the adsorbent-coated rotors used in dehumidification systems, improving performance. In this respect, dynamic sorption properties of MIL-101(Cr) and MIL-100(Fe) in a N_2 gas flow with controlled humidity 60% were scrutinized and compared to commercial adsorbents such as NaX, SAPO-34, and silica gel. It should be noted that the mode of dynamic sorption properties of MIL-101(Cr) and MIL-100(Fe) at 30 °C can also be easily switched

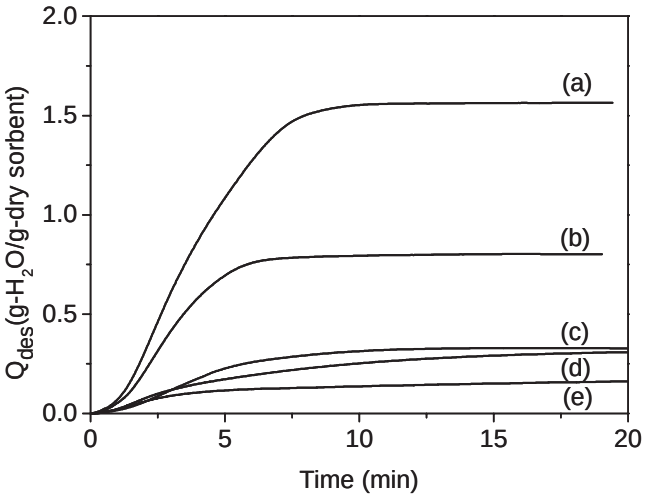

Figure 1. Water desorption profiles of adsorbent materials at 70 °C in a dry N_2 flow: a) MIL-101(Cr), b) MIL-100(Fe), c) silica gel, d) SAPO-34, and e) NaX. Test conditions: temperature-programmed desorption after adsorption at 30 °C and RH 60% for 1 h; ramping rate of desorption: 50 °C min^{-1} from 30 °C to 65 °C and 7.5 °C min^{-1} to 70 °C; and flow rate of N_2 200 mL min^{-1}.

by changing the partial pressure of water (humidity). For example, both the MIL-101(Cr) and MIL-100(Fe) absorb appreciable water at relative humidity (RH) 65% while they could be desorbed at RH 1% at constant temperature (Figure S9, Supporting Information). This corresponds to a room-temperature pressure-swing dehumidification cycle. Dynamic sorption rates of adsorbents of less than 10 min are preferred since adsorbent-coated honeycomb rotors are normally used for desiccant dehumidification systems. Such systems operate by a rotational phase change of adsorption at room temperature and desorption at elevated temperature with a speed of generally 5–30 RPH (revolution per hour).

The desorption rates for these materals at 30 °C are not sufficient for practical dehumidification, so a slight increase of the desorption temperature may be necessary to enhance kinetics. **Figure 1** shows the initial desorption rates of water at 70 °C for materials hydrated at 30 °C using a N_2 carrier gas with a relative humidity 60% (p/p_0 = 0.6). From desorption profiles of the fully hydrated materials, the order of desorption rates is MIL-101(Cr) > MIL-100(Fe) >> silica gel > SAPO-34 > NaX for 10 min. The water desorption capacities for 10 min calculated from the gradients of desorption (desorption rates) in MIL-101(Cr) and MIL-100(Fe) are 1.55 g g^{-1} and 0.797 g g^{-1}, respectively. The capacity in MIL-101(Cr) is 6.0 to 11.5 times higher than those of SAPO-34 and NaX. Moreover, the adsorption rate of MIL-101(Cr) at 30 °C is distinctively higher than those of SAPO-34, NaX, and silica gel (**Figure 2**). The water uptakes for 10 min, estimated from adsorption rate curves in MIL-101(Cr) and MIL-100(Fe) after partial desorption at 70 °C for 10 min are 0.446 g g^{-1} and 0.254 g g^{-1}, respectively (Figure S10, Supporting Information), which are higher than those of SAPO-34, NaX, and silica gel under the same conditions. The poor performances of the zeolites at the desorption stage could be ascribed to their strong hydrophilicities leading to insufficient desorption at low

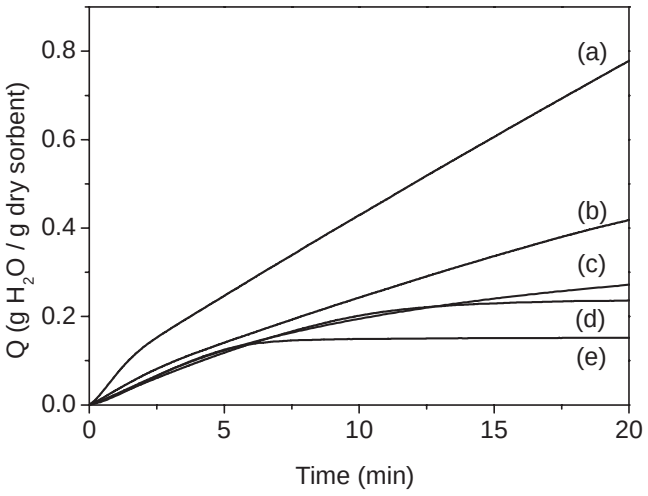

Figure 2. Water adsorption profiles of adsorbent materials at 30 °C in a humid N_2 flow: a) MIL-101(Cr), b) MIL-100(Fe), c) silica gel, d) SAPO-34, and e) NaX. Test conditions: adsorption at 30 °C and RH 60%; and flow rate of N_2, 200 mL min^{-1}.

temperature. Moreover, water adsorption rates of MIL-100(Fe) and MIL-101(Cr) did not change before and after hydrothermal treatments in boiling water at 100 °C for 7 days (Figure S10, Supporting Information), indicating their high durability in water sorption applications. Additionally, ten regeneration cycles of these MILs between adsorption at 30 °C and desorption at 70 °C exhibit essentially no decrease of sorption capacities, within the accuracy of experiments, which further demonstrates the stability under the tested conditions (**Figure 3**, Figure S11, Supporting Information).

Two main reasons could be considered to explain the easier desorption of water compared to purely inorganic porous solids. First, the present MILs are amphiphilic solids since

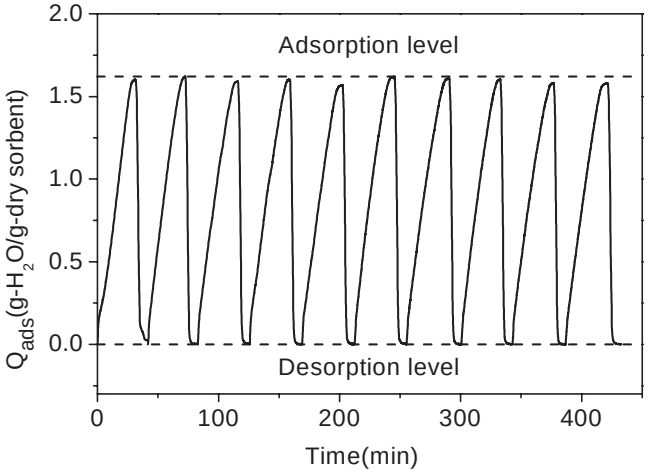

Figure 3. Cyclic operation of water adsorption-desorption for MIL-101(Cr) under a N_2 gas flow. Conditions: adsorption at 30 °C (RH 60%) and desorption at 70 °C (RH < 2%); ramping rate of desorption: 50 °C min^{-1} from 30 °C to 65 °C and 7.5 °C min^{-1} to 70 °C; and flow rate of N_2: 200 mL min^{-1}.

their frameworks are composed of inorganic (metal cations and oxygen anions) and organic moieties (nonpolar carbon atoms and benzene ring) within the pores (**Scheme 1**A). In the as-synthesized form, the terminal molecules on the μ_3-oxo-bridged octahedral metal(III) trimer are two H_2O molecules and, depending on the synthesis conditions, either F^- or OH^- anions.[8] Cages of MIL-100/101 are decorated with 12 oxo-centered trimers, separated by aromatic spacers, with coordinated water molecules in one side and free water molecules in the other side. Secondly, the pores in MIL-100 and MIL-101, while crystalline, are large enough to classify as mesoporous and thus most of the water molecules do not directly interact with the surface of the pores, favoring easier desorption. The large cages (diameter $\Phi \approx$ 24–29 Å) are accessible in MIL-100 through microporous windows ($\Phi \approx$ 5–8.5 Å) and trimers render their coordinated water molecules pointing to their center, which is likely to slow down the diffusion of water. In MIL-101, the larger supermicroporous windows ($\Phi \approx$ 12–16 Å) make the diffusion of water easier. Additionally, the bound water molecules do point not to the center of the windows but to the center of the cages ($\Phi \approx$ 29–34 Å).

Scheme 1 illustrates graphical representations of specific water sorption sites in octahedral trimers of MIL-101 and MIL-100. As evidenced through in situ IR spectra recorded with increasing the temperature under N_2 flow, the terminal water molecules coordinated to trivalent metal cations (1:1 complex, bands at 5280, 3700, and 3605 cm^{-1}) are removable from the respective frameworks by heating above 150 °C under flowing gas (**Figure 4**) or 100 °C under vacuum.[9] The number of the terminal water molecules is theoretically 2.93 mmol g^{-1} (0.05 g g^{-1}) for MIL-101(Cr) and 3.35 mmol g^{-1} (0.06 g g^{-1}) for MIL-100(Fe), which are less than those (0.15–0.20 g g^{-1}) present on the surfaces above 70 °C. It is assumed that the remaining water molecules above 70 °C may be also those that strongly interact with coordinated water molecules as shown in the 4d spectrum (1:2 complex, bands at 5306 and 3680 cm^{-1}).[5b] According to the degree of dehydration between 30 °C and 70 °C, the IR spectra (Figure 4a,b) reveal mainly the presence of both hydrogen-donor (band at ≈3000 cm^{-1}) and electron-donor water molecules (3680 cm^{-1}) in moderate interactions with the terminal water molecules via H-bondings. These H-bonded molecules may exist as extra water multimers forming H_2O—$(H_2O)_n$ chain under a humid N_2 flow. Figure S14 (Supporting Information, MIL-100(Fe)) and Figure S15 (Supporting Information, MIL-101(Cr)) show that the intensity of the 5200–5220 cm^{-1} band, characteristic of the multimer species, depends on the water uptake contrarily to that at 5306 cm^{-1}, characteristic of 1:2 complex, which remains up to 70 °C (Figure 4c). The increase and then the decrease of the bands at 3700 and 3605 cm^{-1} (spectra C to E), assigned to the 1: 1 complex,[5b] show a dynamic water molecule diffusion through the solid upon gas stream at different temperatures, highlighting the progressive dominancy of the most dehydrated entities.

The cumulative enthalpy values of water adsorption for MIL-101(Cr) and MIL-100(Fe) measured by microcalorimetry are correlated with their water sorption uptakes (Figure S17, Supporting Information). Their enthalpy profiles of water adsorption could be apparently divided into two regions. Below about 0.3 g g^{-1} of water adsorption, the profiles correspond

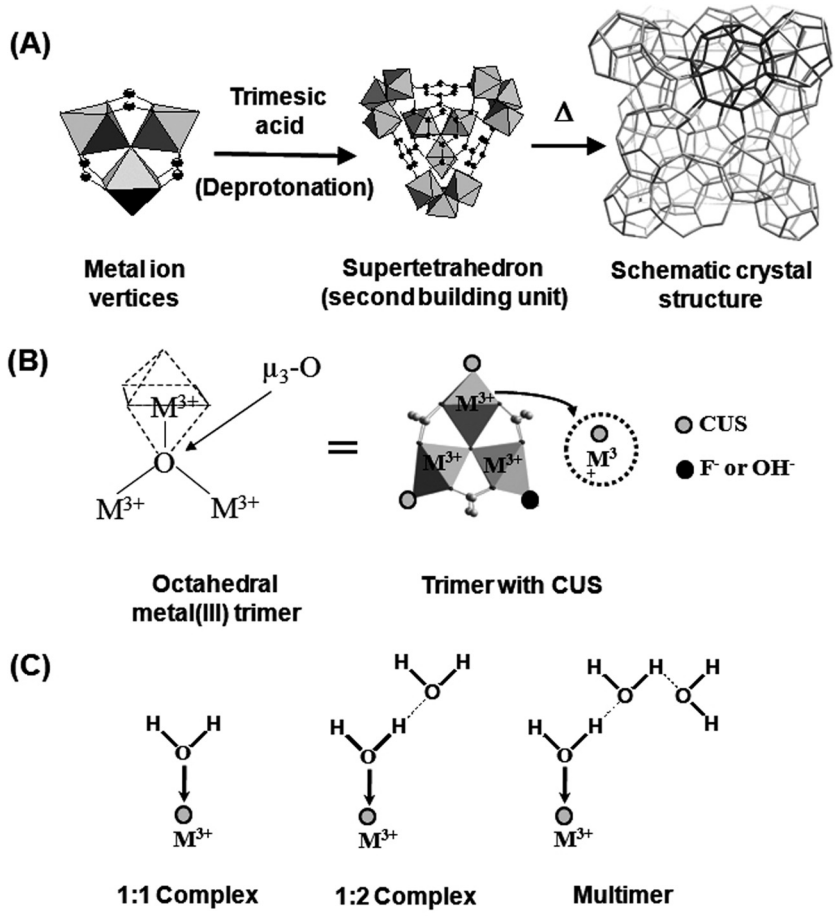

Scheme 1. Graphical representations of specific water sorption sites in octahedral trimers of MIL-101 and MIL-100: A) building units and crystal structure, B) specific water sorption sites in octahedral trimers, and C) metal(III) cation-water complex and H-bonded water multimers.

to a gradual decrease in energy that can be interpreted as the continual adsorption on the coordinatively unsaturated metal cation sites (CUS) and pore surface. This would be attributed to a gradual reorganization of water-adsorbed monolayer. The second region above 0.3 g g^{-1} may correspond to the enthalpies of the capillary condensation in the mesopores, where the enthalpy of adsorption is close to the evaporation enthalpy of water (–40.7 kJ mol^{-1}). For NaX and SAPO-34, the cumulative enthalpy values of water adsorption in the low surface coverage region (<0.03 g g^{-1} of water adsorption) are similar to those for MIL-101(Cr) and MIL-100(Fe) (Figure S18, Supporting Information). However, the integral enthalpies as a function of the relative coverage/filling (= n/n_{sat}) above 0.1 g g^{-1} reveals the following order: NaX > SAPO-34 > MIL-100(Fe) ≈ MIL-101(Cr). In the region close to water saturation on surfaces, the enthalpy values of zeolites (–57.3 kJ mol^{-1} for NaX and –58.3 kJ mol^{-1} for SAPO-34) are distinctively higher than those of MIL-101(Cr) (–44.5 kJ mol^{-1}) and MIL-100(Fe) (–49.5 kJ mol^{-1}). This suggests that most of the water molecules are physisorbed on MIL-101(Cr) and MIL-100(Fe) with a low host–guest interaction (close to the energy of liquefaction) except for the coordinated water molecules, allowing for the low-temperature desorption of water.

Water adsorbents with high sorption capacities and reversible sorption abilities are also very useful for other potential applications such as fresh water production or evaporative humidifiers. In particular, fresh water production that captures moisture from outside air and turns it into pure drinking water is important in many regions that lack safe natural water sources.[10] A general scheme of water production with a solar driven unit as an external energy source for water desorption has been proposed to be effective in desert areas with a hot and dry climate.[10a] Within this report, the accumulated amount of water generated from 3 mm pellets of 10 g MIL-100(Fe) at a simulated condition, i.e., adsorption at 15 °C in humid air (RH 65%) and desorption at 70 °C in less humid air (RH 20%), reaches more than 690 g H_2O per kg dry sorbent per cycle (Figure S19, S20, Supporting Information). This is an intermediate performance between the SiO_2-based[10a] and the MCM-41-based composite sorbents.[10b] Moreover, MIL-100(Fe) is known to be a cheap, biocompatible and nontoxic material that has been utilized as a nanocarrier for drug delivery.[11] The present result implies that the material can be favorably applied to efficient and environmentally friendly production of potable water, especially drinking water.

For a further proof of the possibility of practical adsorptive dehumidification, the large-scale evaluation of honeycomb rotors based on the present adsorbents is underway. Performance results at the initial stage demonstrate that a honeycomb rotor coated with MIL-100(Fe) has almost two times higher efficiency in energy consumption (in terms of input electric power) to operate a test equipment that was

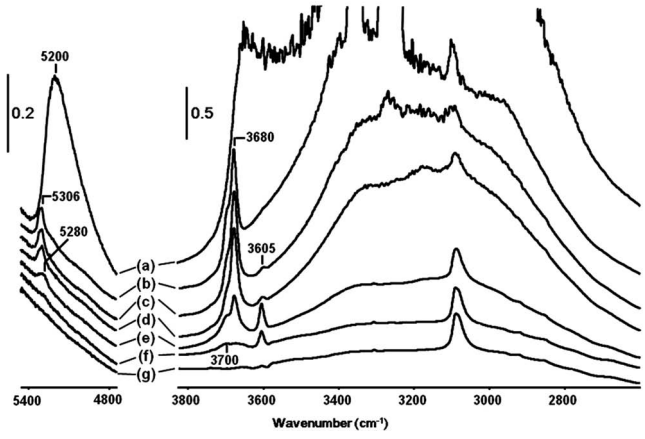

Figure 4. IR spectra of MIL-100(Fe) a) after H_2O adsorption at 25 °C (RH 60% for 1 h) and then heated (1 °C min^{-1}) under N_2 flow at b) 30 °C, c) 70 °C, d) 100 °C, e) 150 °C, f) 200 °C, and g) 250 °C.

designed for a prototype simulation of a household desiccant-type dehumidifier than that with a zeolite rotor, which is commercially available. The detailed results will be published elsewhere.

In conclusion, we have unambiguously demonstrated that hierarchically porous metal–organic frameworks, MIL-100 and MIL-101 with mesoporous cages behave as advanced water adsorbents applicable to energy-efficient dehumidification. Elaborate investigations of their water sorption properties have shown huge sorption uptakes even at 40 °C as well as high desorption rates below 80 °C together with hydrothermal stability. In comparison with the water sorption behaviors of commercial adsorbents such as zeolite NaX, SAPO-34, and silica gel, the improved performance in MIL-100 and MIL-101 demonstrated here suggests commercially viable applications including energy-efficient desiccant dehumidification and fresh water production.

Experimental Section

MIL-100 and MIL-101 were synthesized according to our previous procedures (see Supporting information). The as-synthesized MILs were further purified by two- or three-step treatments using hot water, ethanol, and aqueous NH_4F solutions. IR studies were performed in an infrared Operando cell using self-supported wafers of MIL-101(Cr) and MIL-100(Fe). Operando IR spectroscopic analyses after desorption and adsorption of water vapor as a probe molecule were performed for the identification of adsorbed water species in a He flow or under high vacuum (see Supporting information). The intelligent gravimetric analyzer and thermogravimetric analyzer were used to measure water sorption isobars, isotherms and sorption kinetic curves. Direct measurements of adsorption energies were performed using a Tian-Calvet microcalorimeter coupled to a laboratory-made volumetric device allowing a point by point procedure or a continuous introduction of vapor (see Supporting information).

Supporting Information

Supporting Information is available from the Wiley Online Library or from the author.

Acknowledgements

This work was supported by the international collaboration program (KICOS-MEST, KN-1127) and the Institutional Research Program (KRICT, KK-1101-B0). The French authors acknowledge CNRS for international scientific collaboration program (PICS). S.W. acknowledges the Alexander von Humboldt foundation for his fellowship. The Korean authors also acknowledge Prof. Paul M. Forster, Prof. Sung Hwa Jhung, and CCME members for their helpful assistance.

Received: October 25, 2011
Published online: December 12, 2011

[1] a) R. Z. Wang, R. G. Oliveira, *Prog. Energy Combust. Sci.* **2006**, *32*, 424; b) E.-P. Ng, S. Mintova, *Microporous Mesoporous Mater.* **2008**, *114*, 1; c) J. Jeong, S. Yamaguchi, K. Saito, S. Kawai, *Inter. J. Refrig.* **2010**, *33*, 496.

[2] a) G. Férey, *Chem. Soc. Rev*. **2008**, *37*, 191; b) D. J. Tranchemontagne, J. L. Mendoza-Cortés, M. O'Keeffe, O. M. Yaghi, *Chem. Soc. Rev.* **2009**, *38*, 1257; c) T. Uemura, N. Yanai, S. Kitagawa, *Chem. Soc. Rev.* **2009**, *38*, 1228.

[3] a) A. K. Cheetham, C. N. R. Rao, *Science* **2007**, *318*, 58; b) L. J. Murray, M. Dincă, J. R. Long, *Chem. Soc. Rev.* **2009**, *38*, 1294; c) X. Zhao, B. Xiao, A. Fletcher, K. M. Thomas, D. Bradshaw, M. J. Rosseinsky, *Science* **2004**, *306*, 1012; d) R. E. Morris, P. S. Wheatly, *Angew. Chem. Int. Ed.* **2008**, *47*, 2; e) J. R. Li, R. J. Kuppler, H.-C. Zhou, *Chem. Soc. Rev.* **2009**, *38*, 1477; f) J. Y. Lee, O. K. Farha, J. Roberts, K. A. Scheidt, S. T. Nguyen, J. T. Hupp, *Chem. Soc. Rev.* **2009**, *38*, 1450; g) L. Ma, C. Abney, W. Lin, *Chem. Soc. Rev.* **2009**, *38*, 1248; h) A. C. McKinlay, R. E. Morris, P. Horcajada, G. Férey, R. Gref, P. Couvreur, C. Serre, *Angew. Chem. Int. Ed.* **2010**, *122*, 6400; i) L. Alaerts, C. E. A. Kirschhock, M. Maes, M. A. van der Veen, V. Finsy, A. Depla, J. A. Martens, G. V. Baron, P. A. Jacobs, J. F. M. Denayer, D. E. De Vos, *Angew. Chem. Int. Ed.* **2007**, *46*, 4293.

[4] J. J. Low, A. I. Benin, P. Jakubczak, J. F. Abrahamian, S. A. Faheem, R. R. Willis, *J. Am. Chem. Soc.* **2009**, *131*, 15834.

[5] a) Y. K. Hwang, D.-Y. Hong, J.-S. Chang, S. H. Jhung, Y.-K. Seo, J. Kim, A. Vimont, M. Daturi, C. Serre, G. Férey, *Angew. Chem. Int. Ed.* **2008**, *47*, 4144; b) A. Vimont, J.-M. Goupil, J.-C. Lavalley, M. Daturi, S. Surble, C. Serre, F. Millange, G. Férey, N. Audebrand, *J. Am. Chem. Soc.* **2006**, *128*, 3218; c) J. W. Yoon, Y.-K. Seo, Y. K. Hwang, J.-S. Chang, H. Leclerc, S. Wuttke, P. Bazin, A. Vimont, M. Daturi, E. Bloch, P. L. Llewellyn, C. Serre, P. Horcajada, J.-M. Grenèche, A. E. Rodrigues, G. Férey, *Angew. Chem. Int. Ed.* **2010**, *49*, 5949; d) D.-Y. Hong, Y. K. Hwang, C. Serre, G. Férey, J.-S. Chang, *Adv. Funct. Mater.* **2009**, *19*, 1537.

[6] a) G. Férey, C. Mellot-Draznieres, C. Serre, F. Millange, J. Dutour, S. Surblé, I. Margiolaki, *Science* **2005**, *309*, 2040; b) P. Horcajada, S. Surblé, C. Serre, D.-Y. Hong, Y.-K. Seo, J.-S. Chang, J.-M. Grenèche, I. Margiolaki, G. Férey, *Chem. Commun.* **2007**, 2820; c) G. Férey, C. Serre, C. Mellot-Draznieres, F. Millange, S. Surblé, Julien Dutour, I. Margiolaki, *Angew. Chem. Int. Ed.* **2004**, *43*, 6296; d) C. Volkringer, D. Popov, T. Loiseau, G. Férey, M. Burghammer, C. Riekel, M. Haouas, F. Taulelle, *Chem. Mater.* **2009**, *21*, 5695.

[7] a) J. M. Castillo, T. J. H. Vlugt, S. Calero, *J. Phys. Chem. C* **2008**, *112*, 15934; b) Q. M. Wang, D. Shen, M. Buelow, M. L. Lau, S. Deng, F. R. Fitch, N. O. Lemcoff, J. Semanscin, *Microporous Mesoporous Mater.* **2002**, *55*, 217; c) P. Kuesgens, M. Rose, I. Senkovska, H. Froede, A. Henschel, S. Siegle, S. Kaskel, *Microporous Mesoporous Mater.* **2009**, *120*, 325; d) S. Devautour-Vinot, G. Maurin, F. Henn, C. Serre, T. Devic, G. Férey, *Chem. Commun.* **2009**, 2733; e) L. Grajciar, O. Bludsky, P. Nachtigall, *J. Phys. Chem. Lett.* **2010**, *1*, 3354; f) K. A. Cychosz, A. J. Matzger, *Langmuir* **2010**, *26*, 17198; g) P. D. C. Dietzel, R. E. Johnsen, R. Blom, H. Fjellv, *Chem. Eur. J.* **2008**, *14*, 2389.

[8] a) S. K. Henninger, H. A. Habib, C. Janiak, *J. Am. Chem. Soc.* **2009**, *131*, 2776; b) S. K. Henninger, F. P. Schmidt, H. M. Henning, *Appl. Therm. Eng.* **2010**, *30*, 1692; c) G. Akiyama, R. Matsuda, S. Kitagawa, *Chem. Lett.* **2010**, *39*, 360; d) J. Ehrenmann, S. K. Henninger, C. Janiak, *Eur. J. Inorg. Chem.* **2011**, *2011*, 471.

[9] H. Leclerc, A. Vimont, J.-C. Lavalley, M. Daturi, A. Wiersum, P. L. Llwellyn, P. Horcajada, G. Férey, C. Serre, *Phys. Chem. Chem. Phys.* **2011**, *13*, 11748.

[10] a) Y. I. Aristov, M. M. Tokarev, L. G. Gordeeva, V. N. Snytnikov, V. N. Parmon, *Sol. Energy* **1999**, *66*, 165; b) J. G. Ji, R. Z. Wang, L. X. Li, *Desalination* **2007**, *212*, 176; c) Product information of Munters AB on H_2O LIQUIDAIR, www.muters.us (accessed October 2010).

[11] P. Horcajada, T. Chalati, C. Serre, B. Gillet, C. Sebrie, T. Baati, J. F. Eubank, D. Heurtaux, P. Clayette, C. Kreuz, J.-S. Chang, Y. K. Hwang, P.-N. Bories, L. Cynober, S. Gil, G. Férey, P. Couvreur, R. Gref, *Nat. Mater.* **2010**, *9*, 172.